Polarization dependence of stimulated Brillouin scattering in small-core photonic crystal fibers

John E. McElhenny,* Radha Pattnaik, and Jean Toulouse

Department of Physics, Lehigh University, Bethlehem, Pennsylvania 18015, USA
**Corresponding author: jemm@lehigh.edu*

Received July 3, 2008; revised September 23, 2008; accepted September 23, 2008;
posted October 6, 2008 (Doc. ID 98340); published November 25, 2008

Stimulated Brillouin scattering (SBS) generated from noise in small-core photonic crystal fibers (PCFs) exhibits a strong dependence on pump polarization. The polarization dependence of two small-core PCFs is investigated, yielding unexpected results. Both fibers exhibit birefringence resulting in a 90° polarization dependence for the SBS and a 3 dB difference in the SBS threshold between polarizations corresponding to minimum and maximum SBS, respectively. Surprisingly, the transmission of the smaller-core fiber also exhibits a 180° polarization dependence at lower powers due to polarization-dependent loss. © 2008 Optical Society of America

OCIS codes: 060.4005, 060.5295, 290.5900, 260.5430, 260.1440, 190.5890, 190.4370, 060.4370, 060.0060, 060.2400.

1. INTRODUCTION

Photonic crystal fibers (PCFs), also known as microstructured optical fibers (MOFs) or holey fibers (HFs), have been thoroughly studied over the past decade due to a wide spectrum of possible applications. Consisting of a solid core of pure silica surrounded by a hexagonal array of air holes running along the length of the fiber, solid-core PCFs guide light by an effective total internal reflection mechanism, with the core having a refractive index of 1.44 at 1550 nm and the inner (air–silica) cladding having a lower index between 1.0 and 1.44, depending on the diameter and pitch (center-to-center distance) of the air holes. To manufacture these fibers, a preform is created by arranging small silica capillary tubes (hollow cylinders) in a hexagonal pattern and a fiber is drawn. Thus, the hole diameter (d_h), the lattice pitch (Λ), and core diameter (d_c) can easily be changed, allowing for great flexibility in the design of the fibers and thus in the types of applications. By replacing hollow cylinders with solid cylinders, highly birefringent and polarization-maintaining fibers can also be created [1–3].

Steel *et al.* [4], as well as Koshiba *et al.* [5], have shown theoretically and numerically that perfectly sixfold symmetric hexagonal PCFs are not birefringent. Despite this, Niemi *et al.* [6], Peyrilloux *et al.* [7], and McElhenny *et al.* [8] have observed a characteristic polarization dependence in seemingly symmetric solid-core PCFs. and Peyrilloux *et al.* [7] have studied such fibers theoretically using a finite-element method and experimentally using the magneto-optical method. They have shown that the finite-element method is reliable in predicting birefringence, as long as the grid applied to the cross section of the fiber respects the symmetry of the structure. Accidental birefringence may be caused by material stress and/or fluctuations in the positioning and dimensions of the air holes. Hwang *et al.* [9] have modeled their properties numerically using the plane-wave expansion (PWE) method and found that such unintentional birefringence in PCFs can be suppressed by manufacturing fibers with widely spaced holes (Λ/λ) or small air holes (d/Λ). This, however, may not be suitable for certain applications. Both groups found that birefringence can be induced by nonuniform air hole size, displacement of hole positions, or residual stress. Such birefringence should affect many of the properties of PCFs, particularly the stimulated Brillouin scattering (SBS). The effect of birefringence on the SBS in PCFs, intentional or not, is particularly important since one of their promising characteristics is, in fact, a higher SBS threshold.

To our knowledge, no one has yet studied the polarization dependence of SBS in PCFs, though Stolen *et al.* [10], Spring *et al.* [11], and Yeniay *et al.* [12] as well as others have studied the polarization dependence of SBS extensively in standard single-mode fibers. In this paper, we investigate the unexpected polarization dependence of SBS in two small-core PCFs and the polarization-dependent loss (PDL) [13–15] in the smaller-core fiber of the two. In the next section, we discuss the fiber structure, parameters, and propagation properties. In Section 3, we describe the details of the experimental setup used. Finally, in Sections 4 and 5, we present and analyze the experimental results.

2. FIBER PARAMETERS AND SIMULATIONS

In the present work we study two different fibers: RB65 (6 layers of air holes) from OFS and CF (10 layers) from Crystal Fiber, with core diameters of 3.7 μm and 1.7 μm, respectively. The parameters of these fibers can be found in Table 1 where the core diameter, d_c, is calculated from $d_c = 2\Lambda - d_h$. We also studied a larger core PCF, RB61, with a core diameter of 8 μm but found no polarization dependence.

0740-3224/08/122107-9/$15.00

Table 1. Fiber Parameters and Simulation Results at 1550 nm

Fiber	L (m)	d_h (μm)	Λ (μm)	d_c (μm)	d_h/Λ	Λ/λ	α (dB/km)	n_{eff}	A_{core} (μm^2)	A_{eff} (μm^2)
RB65	384	2.4	3.05	3.7	0.79	1.97	19.4	1.41	10.75	8.07
CF	353	0.72	1.2	1.7	0.60	0.77	71	1.36	2.22	3.0

Simulations using both beam propagation (BeamPROP) and finite element (FemSIM) software showed both fibers to be single-mode. The fundamental modes have an effective refractive index of 1.41 and 1.36 for the RB65 and CF, respectively, using 1.44 for the refractive index of silica at 1550 nm and 1.0 for air. As can be seen in Figs. 1(a) and 1(b), the fundamental mode of the RB65 fiber is confined within the core to an effective area of 8.07 μm^2, while in the CF with a much smaller core of 2.22 μm^2 the fundamental mode extends into the cladding with an effective area of 3.0 μm^2. We revisit this point in Section 5.

It should also be noted that both fibers are highly lossy, with the RB65 having a loss of 19.4 dB/km and the CF a loss of 70 dB/km.

3. EXPERIMENTAL SETUP

The polarization dependence of the SBS was measured using the setup shown in Fig. 2.

A 1550 nm signal from a Photonetics external cavity laser (ECL) was amplified by a 30 dB gain optical amplifier (IPG Photonetics erbium-doped fiber amplifier, model EAD-1-C) and sent through a circulator before entering our polarization control setup. The polarization control component coupled slightly elliptically polarized light into free space using a 10× 0.50 NA microscope objective. In free space, a linear polarizer was used to isolate the linear polarization of the coherent beam before sending it through a half wave plate to control the angle of the linear input polarization. Between measurements, a polarimeter (model PA530) was used after the half wave plate to accurately record the input polarization angle. Using a 20× IR microscope objective, the light was coupled from free space back into the fiber under test (the RB65 or the CF), which was mounted in a high-precision fiber rotator (Thorlabs HFR007) on a translation stage. The rotator was used to align one of the axes of the hexagon with the horizontal axis and only rotated the fibers by 5° to 10° at the outset of the data collection. Once it was at a specified angle, the fiber was not moved for the duration of the measurement. Because there was half a meter between the translation stage and the spool of fiber, this small rotation does not contribute to the birefringence observed. In addition, the same measurements were later repeated without rotating the fiber rotator, and the same polarization dependence was observed. The transmitted power was recorded using a power meter, while the backscattered light traveled back through the polarization control setup and the circulator and onto the lightwave detector (Agilent 20 GHz Lightwave Detector) and electric spectrum analyzer (ESA-L Agilent E4408B). Note that the 3.4 dB loss between the amplifier and the 20× IR microscope objective has already been accounted for in the results reported below.

Three facts should be noted. First, as light is coupled from free space to the flat tip of the fiber, there is strong reflection at the interface (up to 7 dBm reflected through the circulator for an input power of 27 dBm). For input powers close to and below threshold, this strong reflection of the input signal is of the same order of magnitude or higher than the backscattered power. Therefore, the values of the peak powers from our ESA readings were used instead of obtaining the threshold measurements from data collected with a power meter. Thus, the backscattered powers reported are not the absolute powers of the backscattered light but the relative powers, which give an accurate reading of the threshold. This reflection also

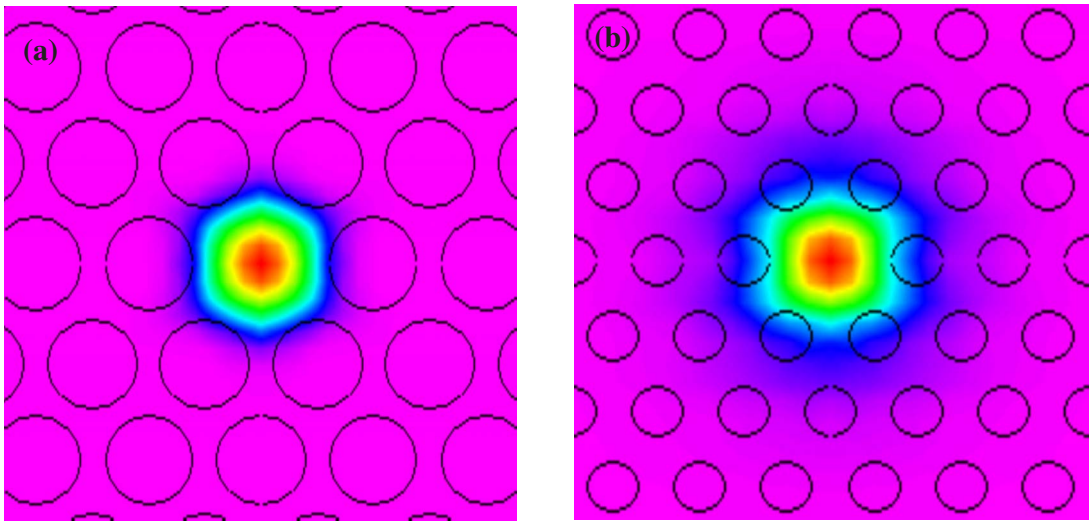

Fig. 1. (Color online) Simulations of fundamental mode of the (a) RB65 and (b) CF fibers using FemSIM.

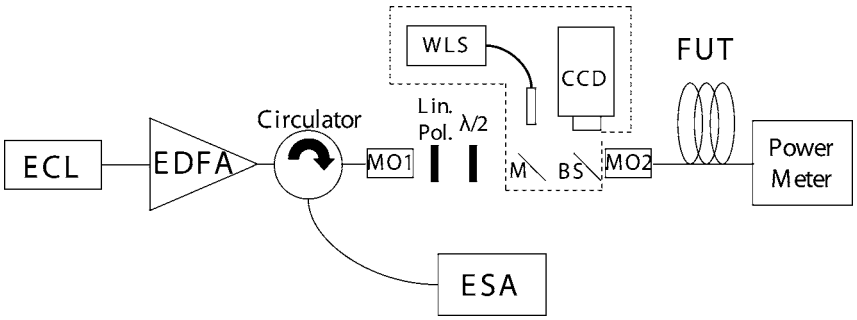

Fig. 2. Configuration of experimental setup to study polarization dependence of SBS. The component in the dotted box was used only to image the fiber tip.

eliminated the need for using the self-heterodyne technique, thereby simplifying the setup.

Second, as mentioned above, the backscattered signal goes back through the polarization component of the system. One may be concerned that this fact itself might cause an artificial change in the polarization dependence observed. This is not the case and was verified theoretically and experimentally. It is well-known that the stimulated backscattered light has the same polarization as the incident light, which is controlled by the polarization setup. If light enters a half wave plate at an angle θ with respect to the wave plate's fast axis, the polarization of the light will be rotated by 2θ. Light propagating back through the wave plate, however, will be rotated by -2θ, resulting in the backscattered light having the same polarization as the input light before it passed through the linear polarizer and into the fiber under test. Experimentally, we verified this by placing a 92:8 polarization insensitive beam splitter (BS) between the half wave plate and the second microscope objective to couple the backscattered light into a fiber and send it to the ESA. Our results showed the same polarization dependence as when the backscattered light travels through the polarization control section.

Finally, we imaged the fiber tip so that the input polarization angle could be determined relative to the orientation of the fiber. The setup depicted in the dashed box in Fig. 2 was used to image the fiber tip. A white light source (WLS) was sent through a 92:8 beam splitter and focused onto the tip of the fiber using a 50× and 100× microscope objective for the RB65 and the CF fibers, respectively. The reflected light was sent back through to the CCD camera where the image of the fiber tip was captured. The images, shown later in Figs. 5(b) and 8(b), have been flipped horizontally as the images were reflected off of the beam splitter before being recorded by the CCD.

4. RESULTS

A. RB65

The Brillouin spectrum for the RB65 fiber is shown in Fig. 3 for two different input polarization angles corresponding to minimum and maximum SBS. The main peak is at 10.96 GHz with a secondary peak about 100 MHz higher. The nature of these multiple peaks is not discussed further here but has been studied earlier by McElhenny *et al.* [8]. For an input power of 23.6 dBm, there is a 40 dB difference between the SBS obtained at the two different polarization angles. This difference can be seen even more clearly in the threshold results below.

The backscattered power, which was recorded using an ESA and not through a direct backscattered power measurement as discussed in Section 3, and the transmitted power are shown in Fig. 4 for four different angles. The input polarization angles resulting in maximum SBS are 13° and 108°, and those resulting in minimum SBS are 60° and −28°. With the input light polarized at angles for maximum and minimum SBS, the threshold powers measured in RB65 are 20.6 dBm and 24.1 dBm, respectively, corresponding approximately to a 3 dB difference as indicated in Fig. 4(a). As will be discussed in Section 5, this is the result that would be expected for a birefringent fiber.

As shown in Fig. 4(b), the transmitted power through the RB65 fiber did not exhibit any polarization dependence for lower powers (below threshold). At higher powers ($P_{in} \geq P_{th}$), a strong polarization dependence is observed with significantly more power (2–3 dBm) transmitted for polarization angles corresponding to minimum SBS than maximum SBS. Obviously, when more power is scattered in the backward direction, less is transmitted through the fiber.

In Fig. 5(a), we plot the peak of the backscattered power vs. the input polarization angle, which reveals the precise polarization dependence of the SBS backscattered light for two different input powers, 21.6 dBm and

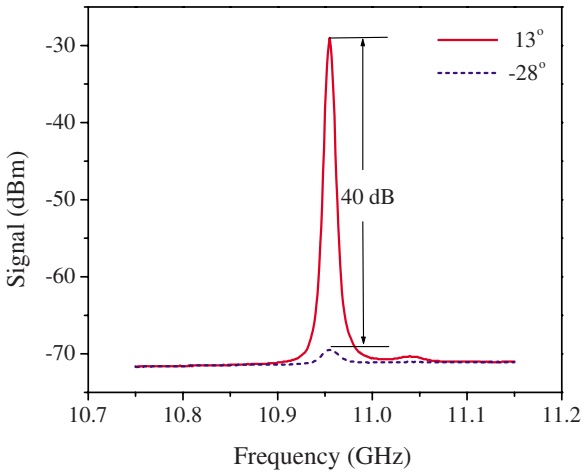

Fig. 3. (Color online) Brillouin signal in the RB65 for an input power of 23.6 dBm and polarization angles of 13° (solid curve) corresponding to maximum SBS and −28° (dashed curve) corresponding to minimum SBS.

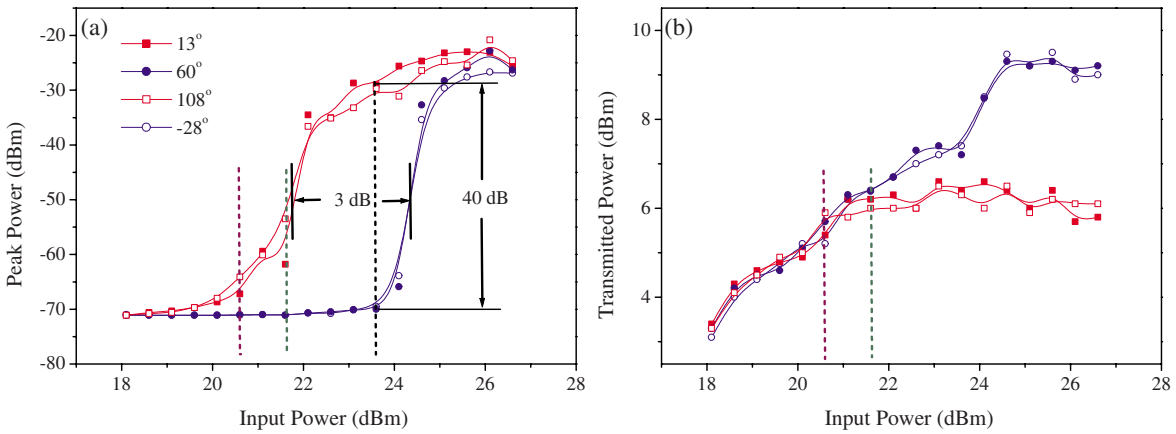

Fig. 4. (Color online) (a) Peak and (b) transmitted powers vs. input power for the RB65 fiber for input polarization angles of 13° and 108° (squares) corresponding to maximum SBS and 60° and −28° (circles) corresponding to minimum SBS. The longer dashed line corresponds the power used in Fig. 3 above and the two shorter dashed lines to the powers used in Fig. 5 below.

22.6 dBm. These powers, corresponding to the data in Fig. 4(a), fall in the region of the threshold for the input polarization angles corresponding to maximum SBS. In Fig. 5(b), the input polarization directions are depicted for maximum and minimum SBS. These angles are shown at 14.75° and 105.5° relative to the horizontal axis for maximum SBS and at angles −29° and 59.5° for minimum SBS. The observed birefringence is rectangular and has its two axes separated by 90°.

As is clear from Fig. 5(b), the polarization angles for maximum SBS do not correspond to the axes of the hexagon, as one might have expected. In fact, according to Steel *et al.* [4] and Koshiba *et al.* [5], PCFs with a perfectly symmetric hexagonal holey cladding should exhibit no polarization dependence.

Finally, when input light was polarized along a principal axis, the output was found to be close to linear and relatively stable. In between the principal axes, the polarization of the transmitted light became more unstable, changing in both ellipticity and orientation over time. Although it could have been interesting to investigate the polarization cross talk, the unstable output prevented such a study.

B. Crystal Fiber (CF)

The CF, with a much smaller core of 1.7 μm, also exhibited very strong polarization dependence as well as unexpected transmission effects. As was the case for RB65, the Brillouin spectrum for the CF (Fig. 6) was found to be polarization-dependent. Here, the main peak is at 10.59 GHz with another peak at 10.96 GHz, approximately 400 MHz from the main peak. These multiple peaks have been studied by McElhenny *et al.* [8]. The peak at 10.96 GHz had the same threshold and exhibited the same polarization dependence as the main peak, though these results are not included. At 24.6 dBm, there is a difference of about 40 dB in the Stokes signal for two different input polarization angles. As with the RB65, this can be seen more clearly in a plot of the backscattered power.

The backscattered and the transmitted powers vs. the input power are shown in Figs. 7(a) and 7(b) for input polarization angles of −39° and 53°, corresponding to the maximum SBS, and of 8° and 97°, corresponding to the minimum SBS. For input polarization angles yielding the maximum SBS the threshold is approximately 21.6 dBm, while for angles yielding the minimum SBS the threshold

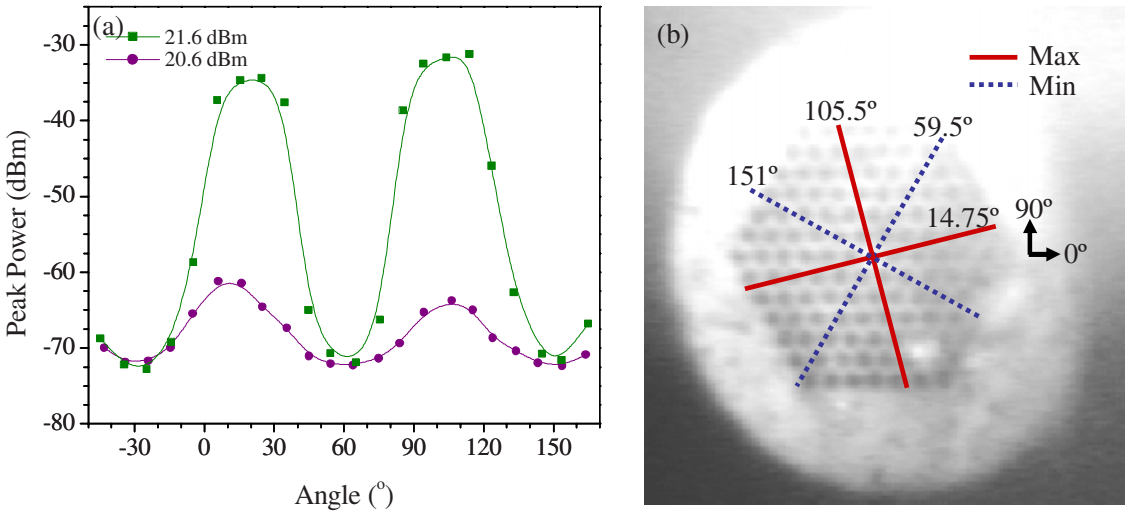

Fig. 5. (Color online) (a) Polarization dependence of SBS in RB65 for two powers, 20.6 dBm (circles) and 21.6 dBm (squares), and (b) the input polarization angles resulting in maximum (solid lines) and minimum (dashed lines) SBS plotted on the image of the fiber tip.

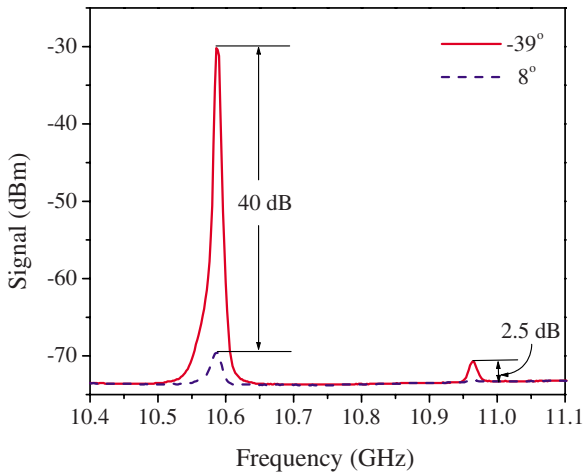

Fig. 6. (Color online) Brillouin signal in the CF for an input power of 24.6 dBm and polarization angles of −39° (solid lines) corresponding to maximum SBS and 8° (dashed lines) corresponding to minimum SBS.

is approximately 24.6 dBm. As with the RB65 fiber, the difference in threshold power for the polarization angles corresponding to maximum and minimum SBS is 3 dB.

The SBS polarization dependence of the CF is presented in Fig. 8. In Fig. 8(a), the backscattered power is plotted against the input polarization angles for two different input powers, 22.6 dBm and 24.6 dBm. The input polarization angles resulting in maximum SBS, 51° and 141°, are 90° apart and do not correspond to the axes of the hexagon but rather indicate rectangular birefringence (shown in Fig. 8(b)). The input polarization angles resulting in minimum SBS, 6° and 96°, are also 90° apart and fall exactly half-way between the two angles for maximum SBS, which thus correspond to the direction of the principal axes.

From Fig. 7(b), it is clear that the transmission of the CF behaves differently than in the RB65. At high powers, above 24.6 dBm (the saturation point for polarization angles of maximum SBS), the transmitted light behaves as expected; there is maximum transmission for minimum SBS and minimum transmission for maximum SBS. However, below saturation, not only is the transmitted light polarization dependent but, for light polarized at −39° (i.e. an angle corresponding to maximum SBS), the transmission is also maximum. When more light is backscattered, more is also transmitted!

This is seen more clearly in Fig. 9, where the transmitted power is plotted against the input polarization angles. The data presented in Fig. 9(a) was taken with all of the previous data presented in this paper and is plotted for the same input powers of 22.6 and 24.6 dBm. It can be seen that 51° corresponds to a minimum in transmission, as expected, but 141° (the other angle for maximum SBS) unexpectedly corresponds to a maximum in transmission. This is quite anomalous as one would expect minimum transmission for both angles resulting in maximum SBS. The angles for maximum transmission are now 180° apart, while those for minimum and maximum SBS are only 90° apart. In a later experiment, for higher input powers (23.9 dBm and 26.2 dBm) and with a different fiber orientation, the transmission shown in Fig. 9(b) does show normal behavior, a correspondence between angles for maximum (minimum) SBS and minimum (maximum) transmission. The earlier results at lower power suggest a polarization-dependent loss, which is confirmed by the transmission curve shown in Fig. 7(b) below threshold. Though the transmitted power behaves differently than in the RB65 fiber, the polarization of the transmitted light behaves the same in both fibers.

5. DISCUSSION

A. Physical Origin of Birefringent Effects on SBS

The experimental SBS results presented for two small-core PCFs show that the intensity of the backscattered Stokes light is at maximum when the incident light is linearly polarized along either one of two axes separated from each other by 90°. The SBS measurements of an elliptical-core fiber reported below in Subsection 5.C also indicate that the maximum SBS corresponds to linear polarization of the incident light along either one of the two principal axes of the elliptical core. Therefore, the two incident linear polarizations that produce maximum SBS in PCFs correspond to the two principal axes of these PCFs.

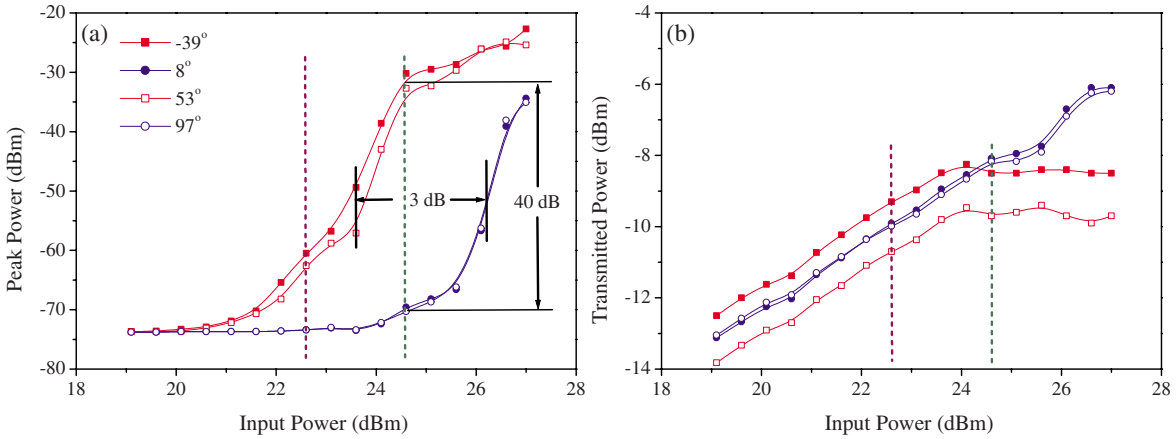

Fig. 7. (Color online) (a) Peak and (b) transmitted powers vs. input power for the CF fiber for input polarization angles of 39° and 53° (squares) corresponding to maximum SBS and 8° and 97° (circles) corresponding to minimum SBS. The dashed lines correspond to the powers used in Fig. 8(a) and 9(a).

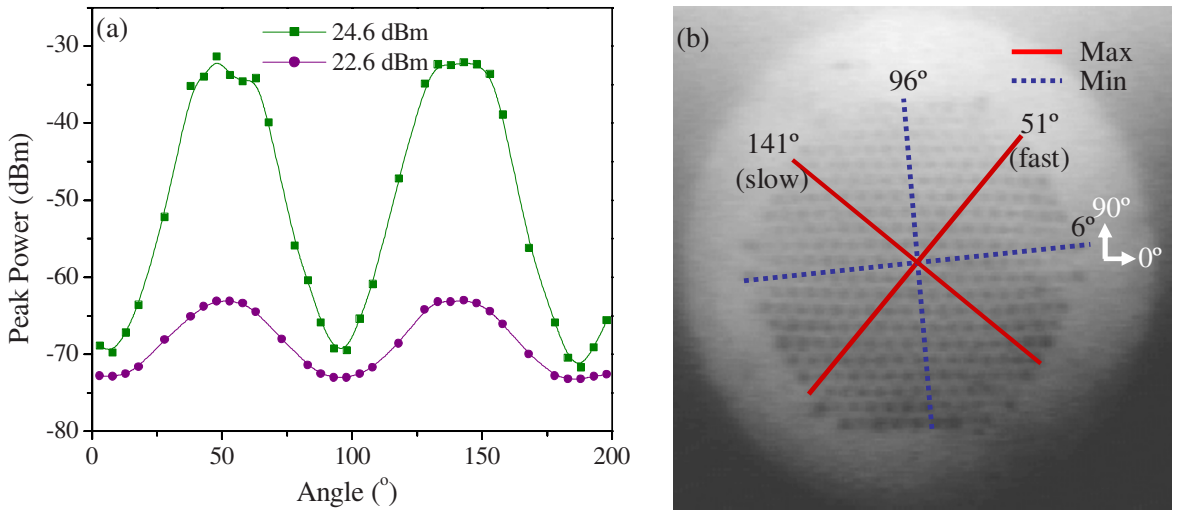

Fig. 8. (Color online) (a) Polarization dependence of SBS in CF for two powers, 22.6 dBm (circles) and 24.6 dBm (squares), and (b) the input polarization angles resulting in maximum (solid lines) and minimum (dashed lines) SBS plotted on the image of the fiber tip.

To further understand the polarization dependence of SBS, we review four well-known facts. First, light at different frequencies experiences different indices of refraction. Second, in a birefringent medium, the difference in refractive index along the two principal axes results in different propagation velocities (slow and fast) along these axes. As such, birefringent fibers maintain linear polarization along the principal axes. Third, at each point in an isotropic medium, the backscattered Stokes light generated at that point assumes the same state of polarization (SOP) as the incident light, irrespective of the particular SOP [11]. Finally, maximum SBS occurs when the incident and Stokes waves have the same SOP [10–12]. If the incident light is linearly polarized along a principal axis, the polarization of both the Stokes and the incident light will be maintained as they propagate, resulting in maximum SBS gain. By contrast, for light polarized midway between the principal axes, the polarization of the pump and Stokes will not be maintained. It will evolve along the length of the fiber becoming elliptically, circularly, and again linearly polarized. If both waves had the same frequency, even though their initial SOPs might not be maintained, the SOP of the Stokes wave would be the same as that of the pump wave throughout the fiber. In other words, the polarization of the Stokes wave, traveling backwards, would go through the same sequence of SOPs that the pump wave had gone through. The polarization of the Stokes wave would retrace the polarization of the pump wave. As such, the SBS gain would be maximum. However, the two waves have different frequencies due to the Doppler effect and thus experience different refractive indices. Thus, their polarization will evolve at different speeds (the Stokes wave will not retrace the polarization of the pump wave) and the two waves will phase out. There will be negligible gain when the wave is completely out of phase (having opposite polarizations) but while it is in phase (same polarization), there will be maximum gain (as in the first case mentioned where the linear polarization of both waves is maintained along the principal axis). Overall, there will be half as much gain as that for maximum SBS, resulting in the threshold power being effectively multiplied by two. This explains the 3 dB change observed in the threshold for the conditions of maximum and minimum SBS respectively. [11]

For example, in the CF, if 24.6 dBm is launched into the fiber at a polarization angle of 141° (i.e. along a principal axis), it remains polarized along this axis, which results in a maximum backscattered power of about

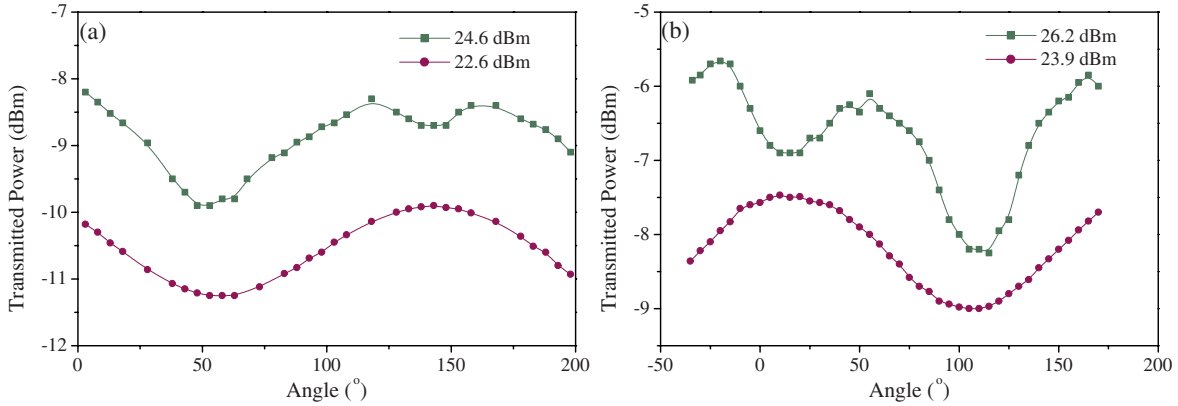

Fig. 9. (Color online) Polarization dependence of the transmitted power in CF for (a) 22.6 dBm (circles) and 24.6 dBm (squares) and (b) 23.9 dBm (circles) and 26.2 dBm (squares), taken at a different time with a different fiber orientation than previous data in the paper.

–30 dBm. However, when light polarized at 96° (45° from the principal axes) is launched, the pump power giving rise to coherent SBS is only half the total power of 24.6 dBm, resulting in 3 dB lower power in each of the two components. Thus, each axis behaves as though the input power were 21.6 dBm, dropping it close to the threshold. The gain is then proportional to only half of the total input power, resulting in a factor of 2 difference from light polarized along a principal axis. By merely changing the input polarization angle away from one of the principal axes, we are thus able to lower the effective input power for SBS such that it falls close to or even below the threshold, thereby reducing SBS significantly.

B. Determination of Fast and Slow Axes

Before analyzing the structural origin of the observed birefringence, determining the fast and slow principal axes is essential. The principal axes are found to be at 14.75° and 105.5° for RB65 and at 51° and 141° for the CF and are shown in Figs. 5(b) and 8(b). In the RB65 fiber, the Brillouin frequency, ν_B, is 10.955 GHz for light polarized at 14.75° and 10.957 GHz for light polarized at 105.5°. The ordinary and extraordinary refractive indices can thus be obtained from $\nu_B = 2\pi n_{\text{eff}} v_A/\lambda$. Light polarized at 14.75° experiences a smaller effective refractive index (and thus a higher velocity) 14.75° corresponds to the fast axis and 105.5° to the slow axis. In the CF, the Brillouin frequency for light polarized at 51° is 10.588 GHz and 10.590 GHz for light polarized at 141°. Thus, in the CF, 51° corresponds to the fast axis and 141° to the slow axis. We now examine the structural origin of these axes.

C. Structural Origin of Birefringence

The curves of the SBS peak powers vs. input polarization angles for the RB65 and CF fibers, in Fig. 5(a) and 8(a) respectively, illustrate the strong birefringent character of small-core photonic crystal fibers. Based on previous work [4,5] a perfectly symmetric PCF with sixfold symmetry should exhibit no birefringence. As these two fibers have a moderate to large d/Λ ratio (0.79 and 0.60 respectively) and a small Λ/λ ratio (1.968 and 0.77 respectively), it follows from Hwang *et al.* [9] that in our small-core fibers either the air-hole structure of the inner cladding is not symmetric (size or position of the holes vary) or the residual stress in the core is not symmetric. Indeed, scanning electron microscope (SEM) pictures of the fiber cross sections (Fig. 10) reveal asymmetries in the hole pattern, especially in the core.

As the optical mode is tightly confined to the core, deformation of the air holes of the innermost ring are of most significance. For RB65, it is clear from Fig. 10(a) that both the size and position of the air holes are nonuniform. The diameter of these air holes varies between 2.24 μm and 2.42 μm, and the spacing between them varies from 0.59 μm to 0.72 μm within an error of 0.02 μm. Most relevant to the observed birefringence is the variation in the core diameter from 3.56 μm to 3.81 μm. These variations indeed result in a slightly elliptical core with an ellipticity of 0.93. Such a break in symmetry resulting in an elliptical core causes the birefringence reported, as we confirm below. Although we have determined the slow axis to be 105.5° from one of the axes of the hexagon and the fast axis to be 14.75° from the same axis in Fig. 5(b), there can be three such orientations in Fig. 10(a), each separated by 60°. Although it is difficult to relate the two pictures, it is still possible to determine the likely alignment of the fast and slow axes. Because the slow axis has the larger refractive index, it follows that it should be expected to lie along the major axis of the elliptical core, while the fast axis will lie along the minor axis.

The CF exhibits similar deformations to the RB65 fiber. The variation in the core diameter (1.85–1.88 μm) and the spacing between the air holes (0.46–0.48 μm) are lower, but at the same time the CF core is significantly smaller and the optical mode therefore extends beyond the strictly silica core. In addition, not only do the air holes vary in size, but they are also more elliptical in shape with the side facing the core of the PCF flattened. Unlike the RB65, the outer regions of the CF's inner cladding are distinct enough so that they can actually be used to match up the axes of the hexagon on the SEM images to those taken with the CCD camera. Thus, the fast and slow axes shown on the SEM image (Fig. 10(b)) are obtained directly from the experimental results. These results logically make sense. The slow axis, which should have the most silica and thus have a higher refractive index, is aligned with the most elongated section of the core (major axis). This supports the assumption that the ex-

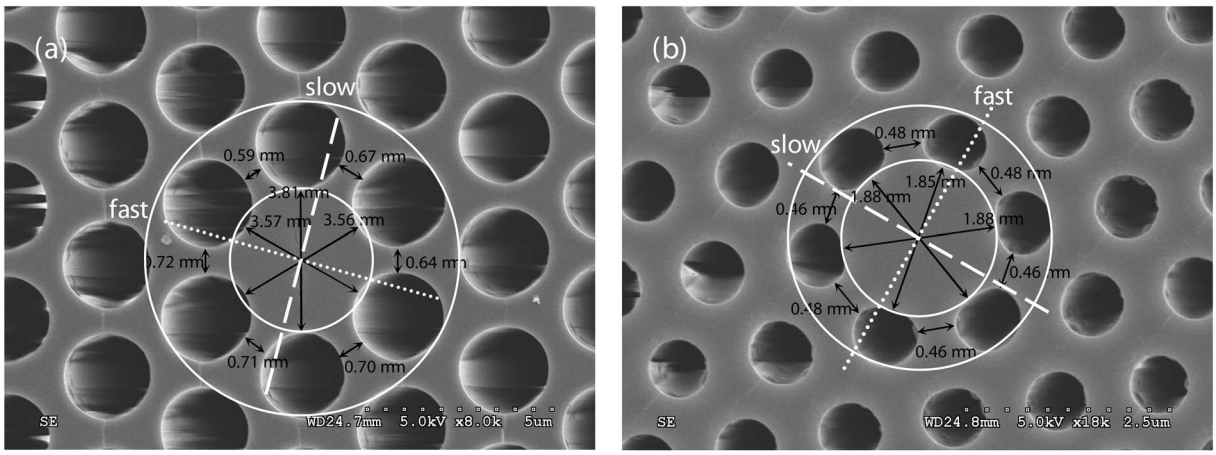

Fig. 10. SEM images of the (a) RB65 and (b) CF fibers. The dotted line is the fast axis and the dashed line is the slow axis.

perimentally observed birefringence is due to a deviation from perfect hexagonal symmetry of the core produced during the drawing process. Though the structural asymmetries in the RB65 are more severe than in the CF, the CF also has a smaller core (and thus a higher intensity) and the optical mode extends further into the cladding, making it more sensitive to smaller asymmetries.

To quantify this birefringence, we look at the difference in the frequency shift between the light polarized along the fast and slow axes ($\Delta f = 1.6$ MHz and 1.8 MHz for RB65 and CF, respectively). The birefringence of the two fibers is calculated (from $\Delta n = \lambda \Delta f / 2c_L$) to be $2.1 * 10^{-4}$ and $2.4 * 10^{-4}$ for the RB65 and CF fiber respectively, using 5900 m/s for the longitudinal velocity of sound in silica. These values are close to the value quoted by Dainese *et al.* [16].

To further show that these small deformations can cause such a large birefringence, we refer to Hwang *et al.* [9]. These authors studied the birefringence induced by varying both the hole position and the hole diameter separately for a fiber with fixed d/Λ of 0.46 and a ratio Λ/λ of 2.1, 6.2 and 10.3. Using only the air holes of the innermost ring and extrapolating their results to estimate the birefringence vs. the variation in hole position to the value Λ/λ of 1.97 and 0.77 of our fibers, the birefringence values of $4 * 10^{-5}$ and $1.8 * 10^{-4}$ are obtained for the RB65 and CF fibers, respectively. Similarly, the birefringence vs. the variation in hole diameter for our fibers yields values of $2.1 * 10^{-5}$ and $2.7 * 10^{-4}$ for the RB65 and CF, respectively. The lower expected birefringence of the RB65 can be explained by the fact that its d/Λ is 0.79, which is much higher than the value of 0.46 used by the authors. They indeed showed that increasing the d/Λ value significantly increases the birefringence.

Similar polarization dependence of the SBS reported here has been observed in polarization-maintaining fibers. One such example is illustrated in Fig. 11 for a solid core/cladding elliptical-core fiber. In this case, the power difference between maximum and minimum SBS was up to 45 dB, comparable to the 40 dB observed for both RB65 and CF fibers. In summary, a very significant birefringence tends to be introduced accidentally in PCFs during the drawing process, primarily due to the weaker mechanical strength of the inner holey cladding. This must be taken into account as it can dramatically change the properties of the PCF, specifically if the polarization of the input light is not controlled. On the other hand, rather than being accidental, a large controlled birefringence could also be introduced purposely in these fibers, through a deformation of the inner cladding, for specific applications.

D. Transmitted Power Through the Crystal Fiber

As discussed in Section 4.B and shown in Fig. 7(b), at powers below SBS saturation more light is transmitted through the CF for input light polarized at 141° than at 51°, indicating a polarization-dependent loss (PDL). This has been numerically demonstrated by Koshiba *et al.* [14] in nonuniform holey fibers. The authors have shown that the field distribution for light polarized along the fast axis mode is less confined than that of the slow-axis mode, resulting in higher loss for light polarized along the fast axis. In the CF, we observe higher loss in transmission for light polarized at 51°. Based on this analysis, 51° must therefore be the fast axis and 141° the slow axis. This indeed is in agreement with our analysis in Section 5.B. As such, light polarized at 141° is more confined, has a lower loss, and thus transmits more light. Because the core of the CF is very small and the fundamental optical mode extends into the cladding (an effective area of 3.0 μm^2 compared to the core area of 2.22 μm^2), changes in the mode field distribution for different polarizations result in higher losses, as we have observed.

6. CONCLUSION

In the present study we have reported experimental evidence of the polarization dependence of SBS in two small-core PCFs. This birefringence is rectangular (twofold symmetric) rather than hexagonal (threefold symmetric) and results in a 3 dB increase in the overall threshold for input light polarized midway between the principal axes. For lower powers, the transmission of the smaller-core CF exhibits a 180° polarization periodicity (unlike SBS, which exhibits a 90° periodicity), which points to polarization-dependent losses. At higher powers, where

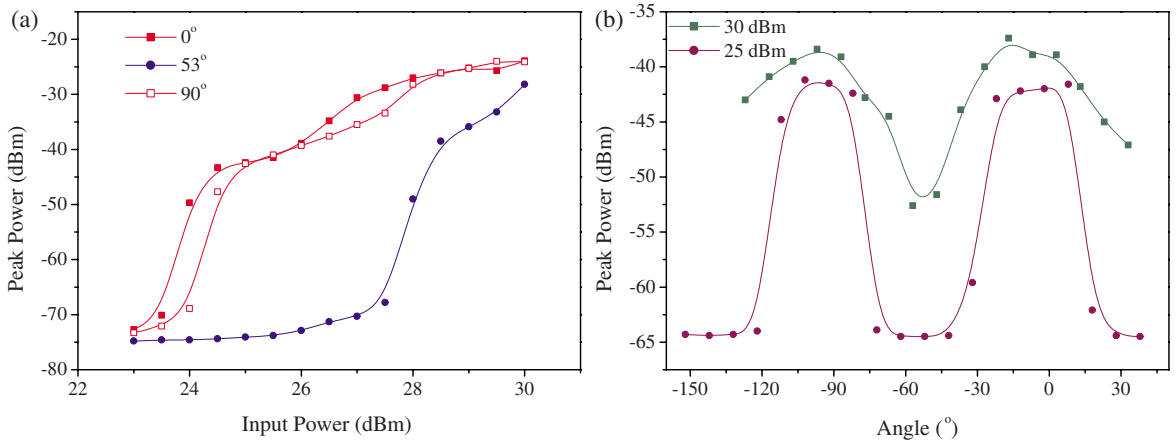

Fig. 11. (Color online) (a) Peak vs. input power for an elliptical core fiber for input polarization angles of along the major and minor axes (squares) corresponding to maximum SBS and at 53° (circles) corresponding to minimum SBS and (b) the polarization dependence of SBS for two powers, 25 dBm (circles) and 30 dBm (squares).

the SBS gain is larger, the PDL becomes negligible and the expected 90° periodicity is recovered for the transmission. The observed strong birefringence is due to asymmetry in the geometrical fiber structure, which even when small is strongly enhanced by both the small-core (and thus high intensities) and the large-index contrast of these PCFs. Such unintentional birefringence in small-core PCFs must be taken into consideration as it can dramatically alter the properties of the PCF, such as raising the threshold by 3 dB and giving rise to polarization-dependent losses. However, it can further increase the appeal of PCFs for applications that are limited by SBS in single-mode fibers.

ACKNOWLEDGMENTS

Special thanks go to Ryan Bise and David Di Giovanni of OFS Inc. for supplying the RB65 fiber studied, as well as Cato Fagermo from Crystal Fiber Inc. for the smaller-core PCF. This work was supported by the National Science Foundation, grant ECS-0401269and by the Center for Optical Technologies at Lehigh Universityfunded by the State of Pennsylvania Department of Community and Economic Development.

REFERENCES

1. A. Ortigosa-Blanch, J. C. Knight, W. J. Wadsworth, J. Arriaga, B. J. Mangan, T. A. Birks, and P. St. J. Russell, "Highly birefringent photonic crystal fibers," Opt. Lett. **25**, 1325–1327 (2000).
2. T. P. Hansen, J. Broeng, S. E. B. Libori, E. Knudsen, A. Bjarklev, J. R. Jensen, and H. Simonsen, "Highly birefringent index-guiding photonic crystal fibers," IEEE Photon. Technol. Lett. **13**, 588–590 (2001).
3. S. B. Libori, J. Broeng, E. Knudsen, A. Bjarklev, and H. R. Simonsen, "High-birefringent photonic crystal fiber," in Proceedings of the Optical Fiber Communication Conference, Vol. 54 of OSA Proceedings Series (Optical Society of America 2001) Paper TuM2.
4. M. J. Steel, T. P. White, C. Martinijn de Sterke, R. C. McPhedran, and L. C. Botten, "Symmetry and degeneracy in microstructured optical fibers," Opt. Lett. **26**, 488–490 (2001).
5. M. Koshiba and K. Saitoh, "Numerical verification of degeneracy in hexagonal photonic crystal fibers," IEEE Photonics Technol. Lett. **13**, 1313–1315 (2001).
6. T. Niemi, H. Ludvigsen, F. Scholder, M. Legré, M. Wegmuller, N. Gisin, J. R. Jensen, A. Petersson, and P. M. W. Skovgaard, "Polarization properties of single-moded, large-mode area photonic crystal fibers," in 28th European Conference on Optical Communication (IEEE, 2002), pp. 1–2.
7. A. Peyrilloux, T. Chartier, A. Hideur, L. Berthelot, G. Mélin, S. Lempereur, D. Pagnoux, and P. Roy, "Theoretical and experimental study of the birefringence of a photonic crystal fiber," J. Lightwave Techol. **21**, 536–539 (2003).
8. J. E. McElhenny, R. K. Pattnaik, J. Toulouse, K. Saitoh, and M. Koshiba, "Unique characteristic features of stimulated Brillouin scattering in small-core photonic crystal fibers," J. Opt. Soc. Am. B **25**, 582–593 (2008).
9. I. K. Hwang, Y. J. Lee, and Y. H. Lee, "Birefringence induced by irregular structure in photonic crystal fiber," Opt. Express **11**, 2799–2806 (2003).
10. R. H. Stolen, "Polarization effects in fiber Raman and Brillouin lasers," IEEE J. Quantum Electron. **QE-15**, 1157–1160 (1979).
11. J. B. Spring, T. H. Russell, T. M. Shay, R. W. Berdine, A. D. Sanchez, B. G. Ward, and W. B. Roh, "Comparison of stimulated Brillouin scattering thresholds and spectra in non-polarization-maintaining and polarization-maintaining passive fibers," Proc. SPIE **5708**, 147–156 (2005).
12. A. Yeniay, J. Delavaux, and J. Toulouse, "Spontaneous and stimulated Brillouin scattering gain spectra in optical fibers," J. Lightwave Techol. **20**, 1425–1432 (2002).
13. W. Urbanczyk, M. Szpulak, G. Statkiewicz, T. Martynkien, J. Olszewski, J. Wojcik, P. Mergo, M. Makara, T. Nasilowski, F. Berghams, and H. Thienpont, "Polarizing properties of photonic crystal fibers," in International Conference on Transparent Optical Networks **2**, 59–63 (2006).
14. M. Koshiba and K. Saitoh, "Polarization-dependent confinement losses in actual holey fibers," IEEE Photonics Technol. Lett. **15**, 691–693 (2003).
15. Y. C. Liu and Y. Lai, "Optical birefringence and polarization dependent loss of square- and rectangular-lattice holey fibers with elliptical air holes: numerical analysis," Opt. Express **13**, 225–235 (2005).
16. P. Dainese, P. St. J. Russell, N. Joly, J. C. Knight, G. S. Wiederhecker, H. L. Fragnito, V. Laude, and A. Khelif, "Stimulated Brillouin scattering from multi-GHz-guided acoustic phonons in nanostructured photonic crystal fibres," Nat. Phys. **2**, 388–392 (2006).